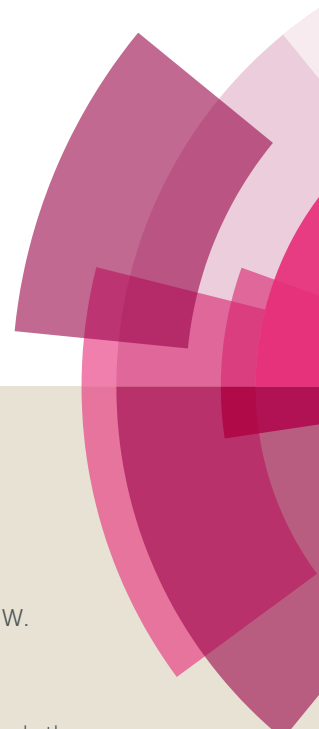


NJC

Accepted Manuscript



This article can be cited before page numbers have been issued, to do this please use: M. El-Shahawi, W. Ahmad, G. I. Mohammed, Y.M. Moustafa, A. El-Asmy and G. Alhazmi, *New J. Chem.*, 2017, DOI: 10.1039/C7NJ00073A.



This is an Accepted Manuscript, which has been through the Royal Society of Chemistry peer review process and has been accepted for publication.

Accepted Manuscripts are published online shortly after acceptance, before technical editing, formatting and proof reading. Using this free service, authors can make their results available to the community, in citable form, before we publish the edited article. We will replace this Accepted Manuscript with the edited and formatted Advance Article as soon as it is available.

You can find more information about Accepted Manuscripts in the [author guidelines](#).

Please note that technical editing may introduce minor changes to the text and/or graphics, which may alter content. The journal's standard [Terms & Conditions](#) and the ethical guidelines, outlined in our [author and reviewer resource centre](#), still apply. In no event shall the Royal Society of Chemistry be held responsible for any errors or omissions in this Accepted Manuscript or any consequences arising from the use of any information it contains.

Impact and correlation of pKa and dn electrons of selected thiosemicarbazone Schiff base metal Co, Ni, Cu complexes: Electrochemical behavior, excitation and optical energies study

M. S. El-Shahawi^{1}, W. Ahmad¹, G.I. Mohammed², Y.M. Moustafa², A.A. El-Asmy³, G.A Al-Hazmi⁴*

¹*Department of Chemistry, Faculty of Science, King Abdulaziz University, P.O. Box 80203, Jeddah 21589, Saudi Arabia*

²*Faculty of Applied Science, Umm Al-Qura University, P.O.Box 16722, Makkah 21955, Saudi Arabia*

³*Department of Chemistry, Faculty of Science, Mansoura University, Mansoura, Egypt*

⁴*Department of Chemistry, Faculty of Science, King Khaled University, P.O. Box 9004, Abha, Saudi Arabia*

*Corresponding author. Tel: 009662-6952000 ext. 644422.; Fax: 009662-6952292,
Email: malsaeed@kau.edu.sa; mohammad_el_shahawi@yahoo.co.uk
On sabbatical leave from the Department of Chemistry, Faculty of Science, Damiatta
University, Damiatta, Egypt.

Abstract

The electron transfer and coordination mechanism of Schiff base with metal ions, correlation of electrochemical and optical properties for their potential applications in various fields of chemistry and biochemistry are underexplored. Thus, detailed assignment of redox behavior of some Co^{2+} , Ni^{2+} and Cu^{2+} thiosemicarbazone complexes in tetrabutylammonium tetrafluoroborate ($\text{TBA}^+ \text{BF}_4^-$)- dimethylformamide (DMF) was investigated by bulk cyclic voltammetry (CV) and controlled potential coulometry (CPC). The redox behavior of the electrode couples (M^+/M^{2+} and $\text{M}^{2+}/\text{M}^{3+}$, $\text{M} = \text{Co}, \text{Ni}$ or Cu) was dependent on the electron donating (or withdrawing) substituent on thiosemicarbazone moiety (N^1H and/or N^4H), Schiff base pKa and d^n electrons of metal ions. On increasing the concentration of the complex species in ($\text{TBA}^+ \text{BF}_4^-$)-DMF, the cyclic voltammograms of the complexes showed no significant variations in the values of the diffusion coefficient(D) $(0.27 - 0.29) \times 10^{-6} \text{ cm}^2 \text{ s}^{-1}$. The E_{pa} and E_{pc} of selected electrode couples were satisfactorily correlated with the remote effect of N^1H and N^4H substituent, Hammett parameters (σ) and d^n electrons of the metal ions. The optical band energies, HOMO and LUMO were obtained from electronic spectra and cyclic voltammogram, respectively. The mechanism describing the electron transfer of the electroactive species and stability of the complex species towards oxidation (M^{3+}) and/ or reduction (M^+) was discussed.

Keywords: Thiosemicarbazone Schiff bases; Redox behavior of Co^{2+} , Ni^{2+} and Cu^{2+} complexes; Ligand pKa; Electrode mechanism; HOMO and LUMO.

1. Introduction

In coordination chemistry, Schiff-bases have often been utilized as chelating ligands [1]. Their potential applications in chemistry, biochemistry, medicine have laid the foundation for its widespread synthesis [2, 3]. They have been used as anti-pyretic, anti-diabetic, anti-bacterial, anti cancer, anti-inflammatory, anti-HIV and as chemosensors [4]. Several Schiff-bases with potential donors N, O and S are helpful in determining transformation mechanism in biological system due to its structural resemblance [5].

Multidentate ligands of thiosemicarbazide and its derivatives containing sulphur and nitrogen have received considerable attention. Their structural, spectral, chemical and redox properties, photochromism, complexing towards heavy metals, catalytic activity and antimicrobial activities are well known [6-13]. Its binding with metal ions may give rise to various coordination modes, thus transforming their biological properties [14]. Regardless of the extensive literature on Schiff bases [6-17], there are still unexplored areas about their coordination mechanism with metal ions, detailed correlation of their electrochemical and optical properties with transition metal ions for their potential applications in various fields. Thus, further studies continued for improving the present day knowledge oriented mainly towards their coordination tendency and biological properties. The redox couples $\text{Co}^{\text{I}}/\text{Co}^{\text{II}}$, $\text{Co}^{\text{II}}/\text{Co}^{\text{III}}$, $\text{Ni}^{\text{I}}/\text{Ni}^{\text{II}}$ and $\text{Ni}^{\text{II}}/\text{Ni}^{\text{III}}$ are markedly affected by the structure of the ligand, stereochemistry of the complex, background electrolyte and nature of solvent [18].

The redox behavior of cobalt (II) and nickel (II) model complexes have special significance as the electron transfer processes in these metals are also involved in many biological systems [19-26]. In continuation to our previous work on thiosemicarbazone Schiff bases and their chelates with Co^{2+} , Ni^{2+} and Cu^{2+} [19-25,27], the present study is focused on: i) Studying the crucial role of pK_a of the Schiff bases on the redox behavior of the observed electrode couples (M^{2+}/M^+ , $\text{M}^{2+}/\text{M}^{3+}$, where $\text{M}=\text{Co}$, Ni or Cu) ; ii) Evaluating the effect of

the of the substituent N¹H and/or N⁴H in thiosemicarbazone moiety of the Schiff bases on the redox properties of metal complexes; iii) Highlighting the properties-structural relationships with the excitation and optical energies of the observed electrode couples of the metal complexes; iv) Investigating the influence of dⁿ - electrons on the E_{pa}, E_{pc}, HOMO, LUMO and optical energies of the observed couples; assigning the most probable reduction mechanism and finally showing the most probable electron transfer mechanism of the electrode couples. This study will be useful for the researchers in understanding the role of the thiosemicarbazone Schiff bases and their metal complexes in biosystems. The study also helps the scientists in assigning the semiconducting properties and the feasibility materials.

2. Experimental

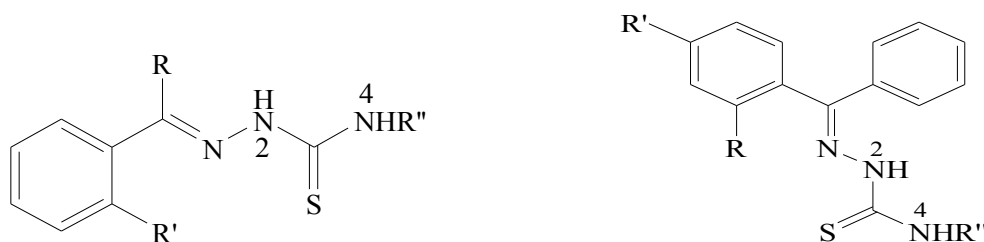
2.1. Reagents and materials

All chemicals and solvents were of A.R. grade. Tetrabutylammonium -tetrafluoroborate (TBA⁺ BF₄⁻) and N, N-dimethylformamide (DMF) were purchased from BDH (Poole, England). The chemical structures are shown in Fig. 1 while the pK_a of the prepared thiosemicarbazone Schiff bases are given in Table 1. The Schiff bases and their cobalt (II), nickel (II) and copper (II) complexes have been prepared and characterized as reported earlier [17-19]. DMF was chosen in the present study as a proper solvent due to its suitable potential window and significant solubility of complexes in this solvent.

Table. 1 Abbreviations, IUPAC names and pK_a values of the of the prepared thiosemicarbazone Schiff bases*

Abbreviation	Name of compound	pK _a value
HAT	1-Acetophenonethiosemicarbazone	11.29
HAET	1-Acetophenone-4-ethylthiosemicarbazone	9.90
HAPT	1-Acetophenone-4-phenylthiosemicarbazone	6.50
HA _p CIPT	1-Acetophenone-4- <i>p</i> -chlorophenyl thiosemicarbazone	8.72
H ₂ ST	1-Salicylaldehydethiosemicarbazone	12.39 (10.05)
H ₂ SET	1-Salicylaldehyde-4-ethylthiosemicarbazone	10.8 (6.1)
H ₂ SPT	1-Salicylaldehyde-4-phenylthiosemicarbazone	10.3 (7.85)
H ₂ SpCIPT	1-Salicylaldehyde-4- <i>p</i> -chlorophenylthiosemicarbazone.	11.3 (8.3)
H ₂ HyMBPT	1-(2-Hydroxy-4-methoxybenzophenone) 4-phenylthio-semicarbazone.	11.5 (4.8)
H ₂ HyMB _p CIPT	1-(2-Hydroxy-4-methoxybenzophenone) 4- <i>p</i> -chlorophenyl thiosemicarbazone.	11.36 (9.3)
HBT	1-Benzophenonethiosimecarbazone.	11.20 (Not available)

*pK_a value of the ligands are taken from reference 14. The values of pK₂ computed by the least square method are given in parentheses.



The abbreviations of R, R' and R'' in the abbreviated Schiff bases are as follows:

HAT : R=CH₃, R', R''=H ;

HAET: R=CH₃, R'=H, R''= -CH₂CH₃

HAPT: R=CH₃, R'=H, R''= -C₆H₅;

HA_pCIPT: R=CH₃, R'=H, R''= 4-ClC₆H₄

H₂ST : R=H, R'=OH, R''=H;

H₂SET : R=H, R'=OH, R''= CH₂CH₃

H₂SPT : R=H, R'=OH, R''= Ph;

H₂SpCIPT: R=H, R'=OH, R''= 4-ClC₆H₄

HBT : R, R', R''= H; H₂HyMBPT: R=OH, R'=-OCH₃, R''=-C₆H₅)

H₂HyMBpCIPT (R=OH, R'=OCH₃, R''= 4 ClC₆H₄)

Fig. 1 Chemical structures of the prepared thiosemicarbazone Schiff bases.

2.2. Physical measurements

Cyclic voltammograms were recorded at room temperature (298 K) on a Potentiostat Wave Generator (Oxford electrode) equipped with Phillips PM 8043 X-Y recorder. A three compartment electrochemical cell configuration consists of Pt wires of 0.5 mm diameter as working and counter electrodes and Ag/AgCl as a reference electrode was used. Anodic (i_{pa}) and cathodic (i_{pc}) peak currents were evaluated [28, 29]. The number of electrons transferred in each electrode processes was determined using controlled potential electrolysis (CPC) in the same supporting electrolyte (DMF-TBA⁺BF₄⁻) at Pt sheet working electrode.

2.3. General preparation of thiosemicarbazone Schiff bases and their complexes (Co, Ni, Cu)

The Schiff bases have been prepared according to the method reported earlier [19-21] as follows: An accurate weight of thiosemicarbazide (9.1 g, 100 mmol) in ethanol was mixed with equimolar amounts of acetophenone, benzophenone and salicylaldehyde individually followed by a reflux for 2-3 h with addition of glacial acetic acid. The precipitates were filtered, recrystallized from ethanol and dried with anhydrous CaCl₂ in desiccators. The stoichiometries and mass data of the prepared Schiff bases are in agreement with the proposed structures (Fig. 1) [19]. Similarly the complexes of cobalt(II), nickel(II) and copper(II) were prepared by adding stoichiometric amounts of ligands and metal acetates followed by reflux for 4-6 h. The formed precipitates were filtered and washed with hot water, ethanol and dried with anhydrous CaCl₂ in desiccators and characterized as reported earlier [19-21].

The purity of the Schiff bases and their Co^{2+} , Ni^{2+} and Cu^{2+} complexes was first tested by TLC using different solvent systems e.g. dioxane-water, acetone-water and petroleum ether at various compositions. Good results were achieved with petroleum ether where well – separated spots were noticed. The sample solution was preconcentrated from 1.0 mL to 10 μL fractions for injection in gas chamber of GC-MS. The products were identified by GC-MS. Total ion chromatogram of the electrolyzed species showed the corresponding significant peak fragments which are most likely corresponding to the proposed chemical structures. The Schiff bases and their complexes were fully characterized as reported earlier [19-24]. The proposed structures were supported by molecular weight determination of the Schiff bases and their complexes. The recorded mass spectra for most of the complexes and the molecular ion peaks confirmed the proposed formulae.

3. Results and discussion

The electrochemical studies for a series of cobalt(II), nickel(II) and copper(II) [24] of complexes thiosemicarbazone Schiff bases have been discussed to highlight the crucial role of pK_a , d^n electrons of the metal ions and structural relationships [18,19]. Considerable advances have been made on studying the biological activity of the thiosemicarbazone Schiff base complexes of the title metal ions. [19, 20]. Thus, most of these complexes have witnessed incredible growth in medicinal chemistry owing to its coordination number, geometries and kinetic properties [17, 20]. These complexes were studied for their redox behavior and it confirmed that they can be used efficiently for treatment of tuberculosis (TB) [22].

3.1. Redox behavior of cobalt (II) complexes

The electrochemical parameters of mono and bi-nuclear cobalt (II) complexes in $\text{DMF-TBA}^+.\text{BF}_4^-$ are given in Table 2. Representative cyclic voltammograms of the binuclear

complex $[\text{Co}_2(\text{SET})_2]\cdot\text{C}_2\text{H}_5\text{OH}$ is also shown in Fig.2. In general, the CVs of the cobalt(II) complexes reveal diffuse, irreversible and successive two one –electron reductions coupled with two one –electron oxidation. The irreversible nature of the cathodic peaks was confirmed by the large potential-potential difference ($\Delta=E_{\text{pc}}-E_{\text{pa}}$) between two counter peaks or the absence of well defined peaks in the reverse scan. By increasing the potential scan rates (ν) from 0.01 to 1 V s^{-1} , response were achieved in which the ($i_{\text{p,a}}/i_{\text{p,c}}$) ratio for the observed couples ($\text{Co}^{2+}/\text{Co}^{3+}$ and $\text{Co}^{2+}/\text{Co}^+$) progressively decreased. Thus, the mass transfer is limited and the species that initially formed in the electrode process may also react further to give products that are not reoxidized at the same potential as the first formed species. At $\nu > 1.0 \text{ V s}^{-1}$, the responses were typical of an uncomplicated one-electron charge transfer whose nature appeared not typical reversible from the CVs explored at high sweep rate.

The CVs of the mononuclear cobalt(II) complexes: $[\text{Co}(\text{AET})_2(\text{H}_2\text{O})_2]$, $[\text{Co}(\text{APT})_2(\text{H}_2\text{O})_2]$, $[\text{Co}(\text{SPT})(\text{H}_2\text{O})]$, $[\text{Co}(\text{SpClPT})(\text{H}_2\text{O})_2]\cdot\text{H}_2\text{O}$ and $\text{Co}(\text{HyMBPT})(\text{H}_2\text{O})_3]\cdot\text{H}_2\text{O}$ displayed two electrode couples. The cyclic voltammograms showed two cathodic peaks (E_{pc}) in the range $-0.98 - 0.07 \text{ V}$ (E_{pc1}) and $-0.21 - 0.92 \text{ V}$ (E_{pc2}) coupled with two anodic peaks (E_{pa}) in the range $-0.3 - 0.14 \text{ V}$ (E_{pa1} , couple I) and $0.04 - 1.02 \text{ V}$ (E_{pa2} , couple II), respectively. The ΔE_{p} values (where $\Delta=E_{\text{pc}}-E_{\text{pa}}$) of the couples were found higher than 60 mV except for $\text{Co}(\text{HyMBPT})(\text{H}_2\text{O})_3]\cdot\text{H}_2\text{O}$ (Table 2) suggesting the irreversible nature of the electrode couples. The cyclic voltammogram of the complex $\text{Co}(\text{HyMBPT})(\text{H}_2\text{O})_3]\cdot\text{H}_2\text{O}$ showed $E_{\text{pc}} = -0.36\text{V}$ coupled with $E_{\text{pa}} = -0.30 \text{ V}$ with $\Delta E_{\text{p}} \cong 60 \text{ mV}$ indicating the reversible nature of the couple. By analogues with the cyclic voltammograms of other cobalt(II) complexes [20-23], the first couple (couple I) was safely assigned to $\text{Co}^+/\text{Co}^{2+}$ couple whereas the second couple (couple II) couple was assigned to $\text{Co}^{2+}/\text{Co}^{3+}$. In the same potential window ($-1.0-1.0 \text{ V}$), the CVs of the Schiff bases were also recorded to rule out the possible presence of redox peaks of imine and thiocarbonyl groups present in the ligands. The CVs results revealed no E_{pa} or

E_{pc} in the employed potential window at the used scan rate (50-100 mVs^{-1}) confirming the observed electrode couples of cobalt ($\text{Co}^{2+}/\text{Co}^{3+}$ and $\text{Co}^{2+}/\text{Co}^{+}$).

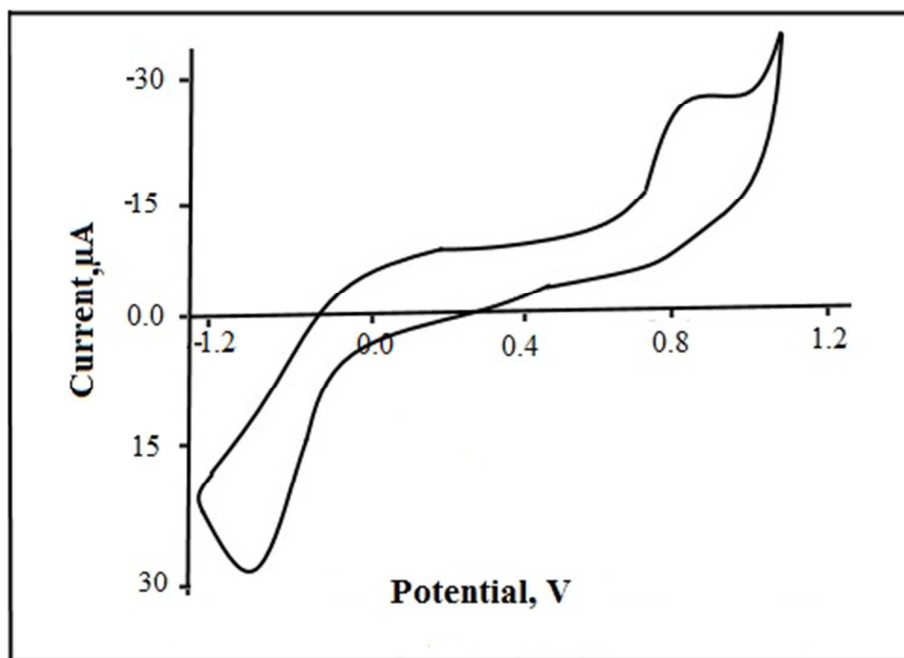


Fig. 2 Cyclic voltammogram of $[\text{Co}_2(\text{SET})_2]\text{C}_2\text{H}_5\text{OH}$ in $\text{TBA}^+\text{BF}_4^-$ -DMF- at 100 mVs^{-1} vs. Ag/AgCl reference electrode.

Controlled potential coulometry (CPC) at Pt net electrode of the complex

$[\text{Co}(\text{HyMBPT})(\text{H}_2\text{O})_3]\cdot\text{H}_2\text{O}$ was recorded at the potential of the limiting current plateau of the cathodic peak under N_2 atmosphere. The number of electron transfer was calculated from the charge – time curve using the following equation [30]:

$$Q_F = Q_T - Q_B = n FVC \quad (1)$$

where Q = charge in coulomb, Q_F = the faradic charge required for complete electrolysis of the complex in solution, Q_T = the faradic charge required for complete electrolysis of the test solution which was measured by extrapolating the linear of the curve to zero time, Q_B = the faradic charge required for complete electrolysis of the supporting electrolyte only, V = volume of the test solution in the cell in liter, C = the concentration of the solution, mol L^{-1}

and $F =$ Faraday's number (96485 C/equiv). At the potential of the limiting current plateau of E_{pc} of Co^{2+}/Co^{+} couple of $[Co(HyMBPT)-(H_2O)_3] \cdot H_2O$, the data confirmed one electron transfer/one cobalt centre in the complex.

The linear dependence of E_{pc} vs. scan rate ($\log v$) for the couple Co^{2+}/Co^{+} of the complex of $[Co(AET)_2(H_2O)_2]$ (Fig. 3) confirmed the irreversible nature of the reduction step. From the slope of this plot, the product of the number (n) of electrons involved in the reduction step and the corresponding charge transfer coefficient (α) can be determined. Assuming $n=1$, and α value of 0.68 is obtained. The values of E_{pa} and E_{pc} of this couple (Co^{2+}/Co^{+}) were also shifted to more positive and negative values, respectively adding further support to the irreversible nature of the couple [29,31].

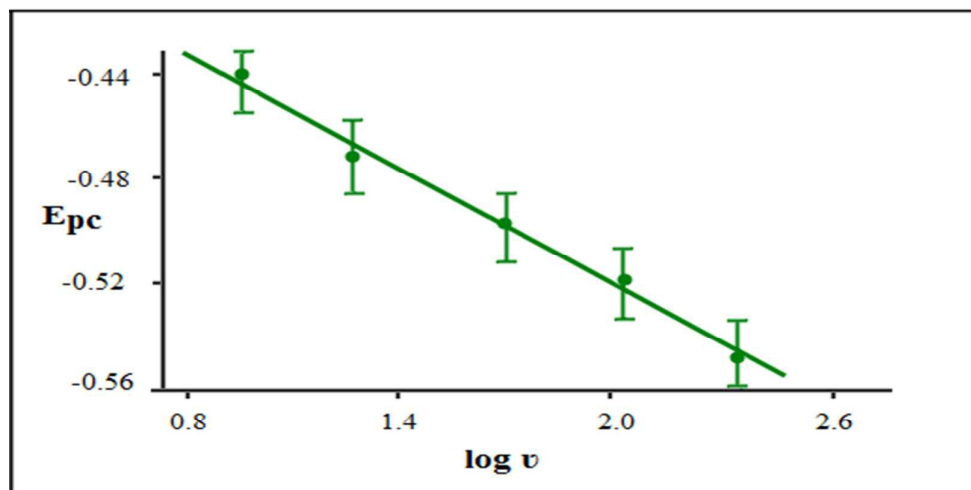


Fig. 3 Plot of $E_{p,c}$ vs. $\log v$ for the electrode couple Co^{2+}/Co^{+} of the complex $[Co(AET)_2(H_2O)_2]$, vs. Ag/AgCl electrode.

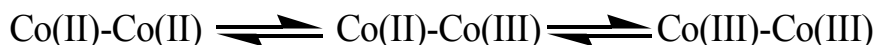
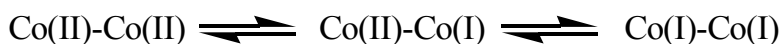
The peak current ($i_{p,c}$) of the couple Co^{2+}/Co^{+} is directly proportional to the square root of the potential sweep ($v^{1/2}$) and the plot of $i_{p,c}$ vs. v was linear and passing through the origin of coordinates.

At the temperature used and according to the CV theory [28, 29], this electrode process is controlled by diffusion up to the polarization of sweep rate. Based on these results and the

peak current of other cobalt(II) complexes [22,23], couple I was safely assigned to the irreversible couple $\text{Co}^{2+}/\text{Co}^+$. The current function ($i_{p,c}/\nu^{1/2}$) of $\text{Co}^{2+}/\text{Co}^+$ couple decreased linearly on increasing concentration of the complex ion. On the other hand, similar trend was also noticed on raising the sweep rate confirming an EC type mechanism in which an irreversible first order reaction is proposed [31, 32].

The cyclic voltammogram of $[\text{Co}(\text{HyMBPT})(\text{H}_2\text{O})_3]\cdot\text{H}_2\text{O}$ showed another couple with E_{pa} in the range of 0.04-1.2 V coupled with an ill defined peak E_{pc} in the range of -0.21 to +0.92 V vs. Ag/AgCl electrode. CPC measurement at the potential of the limiting current plateau of $E_{p,c}$ of this couple showed an indication of one electron transfer/cobalt center. Thus, the couple was safely assigned to the irreversible one electron oxidation ($\text{Co}^{2+}/\text{Co}^{3+}$). The value of ΔE_p of this couple was found in the range 60 ± 7 mV at $\nu < 100 \text{ mVs}^{-1}$ and it increased at $\nu \geq 100 \text{ mVs}^{-1}$. On raising the sweep rate, the complex species that are initially formed during the reduction process may be changed to some other forms (or decomposed to products) that are not re-oxidized at the same potential [31-33]. The kinetics of follow up chemical reactions at $\nu > 100 \text{ mVs}^{-1}$ may also lead to different products of electrogenerated Co^{3+} complex species that influence the peak current ratio [31, 32].

The cyclic voltammograms of the binuclear complexes $[\text{Co}_2(\text{AT})_3(\text{OH})(\text{H}_2\text{O})_2]2.5\text{H}_2\text{O}$, $[\text{Co}_2(\text{ApCIPT})(\text{OAc})(\text{OH})_2(\text{H}_2\text{O})]\text{H}_2\text{O}$, $[\text{Co}_2(\text{ST})_2(\text{H}_2\text{O})_2]0.5\text{H}_2\text{O}$, $[\text{Co}_2(\text{SET})_2]\text{C}_2\text{H}_5\text{OH}$ and $[\text{Co}_2(\text{HyMBpCIPT})(\text{OH})_2(\text{H}_2\text{O})_3]$ (Table 2) showed two successive two one - electron reduction processes. In the reverse scan, two successive one electron oxidation couples were easily observed. Based on the sequential one electron transfer for $\text{Co}^{2+}/\text{Co}^+$ and $\text{Co}^{2+}/\text{Co}^{3+}$ couples of other similar binuclear cobalt(II) complexes [32-35], the observed trend in the complex $[\text{Co}_2(\text{ST})_2(\text{H}_2\text{O})_2]0.5\text{H}_2\text{O}$ can be assigned to the sequential one electron transfer reactions as demonstrated in scheme I.



Scheme I. Proposed sequential one electron transfer mechanism for the binuclear cobalt (II) complexes.

The chemical structures of Co^+ or Co^{3+} complex species, hence can easily be deduced by adding and/ or withdrawing one electron in the form of H^+ or H^- to cobalt (II) in the complex species (Fig. 4), respectively.

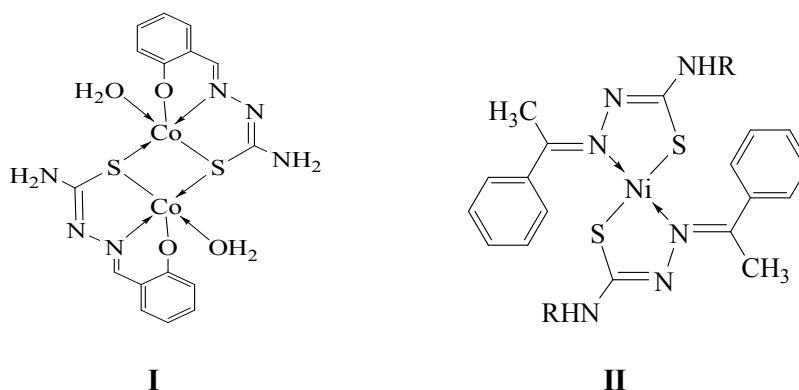


Fig.4. Proposed chemical structures of the complexes $[\text{Co}_2(\text{ST})_2(\text{H}_2\text{O})_2]_{1/2}\text{H}_2\text{O}$, **I** and $[\text{Ni}(\text{AET})_2]$, **II**.

The values of E_{pc} of the couple $\text{Co}^{2+}/\text{Co}^+$ of the binuclear cobalt(II) complexes were found less negative than that of the mononuclear ones in agreement with data reported for other cobalt(II) complexes [33, 34] (Table. 2). Thus, the ability of the mononuclear complex species to accept electron is much easier compared to the binuclear ones and these E_{pc} values are in agreement with the data reported for other cobalt(II) complexes [33, 34]. The constancy of the $i_{p,c}/i_{p,a}$ ratios at the employed scan rate ($\nu = 20\text{-}200$ mV/s) confirmed the stability of the single one-electron reduction of the couple $\text{Co}^{2+}/\text{Co}^+$ of the binuclear ones. The variation of the current function ($i_{p,c}/\nu^{1/2}$) of this couple decreased continuously with the scan rate (>500.0 mVs $^{-1}$), revealing that, the reduction process favors ECE (chemical

reaction coupled between two charge - transfer processes) type mechanism and adsorption of the electroactive species is limited [27-29].

Table. 2 Electrochemical data (V) of cobalt (II) complexes in DMF-TBA⁺BF₄⁻ vs. Ag/AgCl reference electrode at 100 mVs⁻¹*

Complex	Electrode couple, I			Electrode couple, II		
	E _{pa}	E _{pc}	ΔE _p	E _{pa}	E _{pc}	ΔE _p
[Co ₂ (AT) ₃ (OH)(H ₂ O)]2.5H ₂ O	0.46	-0.62	1.08	0.60	0.36	0.24
[Co ₂ (AT) ₃ (OH)(H ₂ O)]2.5H ₂ O	-0.17	+0.07	0.10	0.84	0.70	0.14
[Co(AET) ₂ (H ₂ O) ₂]	-0.20	-1.27	1.07	0.75	0.49	0.26
[Co(APT) ₂ (H ₂ O) ₂]	-0.22	-0.67	0.45	1.02	0.92	0.10
[Co ₂ (ApCIPT)(OAc)(OH) ₂ (H ₂ O)]H ₂ O	-0.54	-0.60	0.06	0.10	0.04	0.05
[Co ₂ (ApCIPT)(OAc)(OH) ₂ (H ₂ O)]H ₂ O	-0.26	0.33	0.07	0.63	0.57	0.06
[Co ₂ (ST) ₂ (H ₂ O) ₂]0.5H ₂ O	0.62	-0.51	1.13	1.38	0.34	1.04
[Co ₂ (SET) ₂]C ₂ H ₅ OH	-0.50	-0.98	0.48	0.72	0.64	0.08
[Co ₂ (SET) ₂]C ₂ H ₅ OH	-0.20	0.26	0.06	0.88	0.80	0.08
[Co(SPT)(H ₂ O)]	0.14	-0.84	0.98	0.80	-0.21	1.01
[Co(SpCIPT)(H ₂ O) ₂]H ₂ O	-0.18	-0.96	0.78	0.88	0.03	0.85
[Co(HyMBPT)(H ₂ O) ₃]H ₂ O	-0.30	-0.36	0.06	0.04	-0.06	0.10
[Co ₂ (HyMBpCIPT)(OH) ₂ (H ₂ O) ₃]	-0.38	-0.44	0.06	0.54	0.34	0.20
[Co ₂ (HyMBpCIPT)(OH) ₂ (H ₂ O) ₃]	+0.01	0.05	0.06	0.86	0.80	0.06

$$*\Delta E_p = E_{pc} - E_{pa}$$

The influence of varying concentrations of [Co₂(AT)₃(OH)(H₂O)]2.5H₂O (as a representative example of cobalt(II) binuclear complexes) on the values of E_{pc} and diffusion coefficient (D) of the couple Co²⁺/Co was also studied. On raising the concentrations from 1.0×10⁻⁴ to 4.0×10⁻³ mole/dm³, the value of E_{pc} was shifted cathodically adding further support to the irreversible nature of the couple. The value of D of the couple was also calculated using the equation [36, 37]:

$$i_{p,c} = 2.72 \times 10^5 n^{3/2} D^{1/2} C^0 v^{1/2} \quad (2)$$

where $i_{p,c}$ = cathodic peak current ($A\ cm^{-2}$), n =number of electrons involved in the electrochemical step, v is the scan rate (V/s^{-1}) and C^0 is the concentration of the depolizer complex ($mmole/dm^3$). On raising the concentration of the depolizer, the computed values of D were found in the range of $(0.27 - 0.29) \times 10^{-6}\ cm^2\ s^{-1}$. These variations were not very significant suggesting no aggregation behavior of the complex species in the solution [36-38]. The trend of other cobalt(II) complexes may also be rationalized in a similar approach.

A comparison between mononuclear cobalt(II) mononuclear complexes $[Co(AET)_2(H_2O)_2]$, $[Co(APT)_2(H_2O)_2]$, $[Co(SpCIPT)(H_2O)_2]H_2O$ and $[Co(SPT)(H_2O)]$ is given in Table 2. The comparison was based on taking two variables into consideration i.e the influence of the nature of the bulky group and the influence of the position of the bulky group on both the complexes. The data given in Table 2 revealed that, the electron-withdrawing group (p -ClC₆H₄) makes the former complex ($[Co(SpCIPT)(H_2O)_2]H_2O$) more positively charged and easy to be reduced (Table 2) more than the latter one ($[Co(SPT)(H_2O)]$) containing electron donating group (phenyl) (Table 2). Hence, cobalt(I) species are stabilized by electron-withdrawing groups whereas cobalt(III) species are stabilized by electron-donating groups. The influence of the Schiff base pK_a , on the values of E_{pa} and E_{pc} of the couple Co^{2+}/Co^+ of a series of selected cobalt(II) complexes with different substituent groups on the thiosemicarbazone moiety N^1H and/ or N^4H was critically determined. The values of E_{pa} and E_{pc} are not simply correlated to the pK_a values (where K_a =acid dissociation constant) of the ligands. The influence of the change of the coordination number of the ions upon the redox potentials may account for this trend [39]. The E_{pa} and E_{pc} values of an electrochemically irreversible system depends on the chemical kinetics involved in the electron transfer process. Thus, the value of $E_{1/2}$ i.e. $(E_{pa}+E_{pc})/2$ has no thermodynamic meanings [27-29]. The E_{pa} and E_{pc} values were not very sensitive to the change in the nucleophilic properties of the

azomethine nitrogen atom of the thiosemicarbazone moiety N^1H and/ or N^4H substituent in the ligand (Table 2). The substitution by the ethyl or phenyl group on N^4H on $[Co(AET)_2(H_2O)_2]$ and $[Co(APT)_2(H_2O)_2]$ complexes makes both oxidation and reduction processes more difficult than other complex species. This effect may be explained by a steric effect of the ethyl or phenyl group at the reduction centre, which would hinder the approach of the reduction centre to the surface of the Pt electrode [40]. The potential generated by the electron density of the donor atoms on the anti-bonding d orbital is also participated and responsible for the observed trend [33, 38]. Thus, cobalt chelates of ligands of high electron density on their donor atoms showed lower E_{pa} and E_{pc} values compared to other Schiff bases of lower pK_a .

3.2. Redox behavior of nickel (II) complexes

The cyclic voltammograms of the square planar nickel(II) thiosemicarbazones complexes in the potential range of -1.2 to +1.2V vs. Ag/AgCl at 100 $mV s^{-1}$ displayed two electrode couples. The electrochemical parameters are given in Table. 3 and representative cyclic voltammogram of the complex $[Ni(H_2SpCIPT)(OAc)_2(H_2O)]$ at 100 $mV s^{-1}$ scan rate is shown in Fig. 5. CPC at potential lower than $E_{p,c}$ (-0.45 to -1.25 V) revealed that, the species are reduced via one electron/ nickel center. The one electron nature of this couple (Ni^{2+}/Ni^+) was also established by comparison with other nickel (II) analogs [34].

Electrochemical data for Nickel (II) complexes of the Schiff bases H_2ST , H_2SET , H_2SPT , $H_2SpCIPT$, $H_2HyMBPT$ and $H_2HyMBpCIPT$ (Table 3) showed similar trend. Changing the scan rate from $\nu = 20$ to 200 $mV s^{-1}$, showed an ill (not well resolved) defined cathodic peak with $E_{p,c}$ in the range -0.82 – to 1.09 V coupled with one anodic peak (E_{pa}) in the -0.04 – -0.67 V with $\Delta E_p = 0.31 - 0.79$ V. The values of $E_{p,c}$ and $E_{p,a}$ shifted cathodically and anodically, respectively on increasing the potential sweep confirming the irreversible nature

and occurrence of slow electrochemical reaction following the electrode process [41]. The influence of the sweep rate on the anodic peak current of cyclic voltammogram of the complex $[\text{Ni}(\text{HHyMBPT})(\text{OH})(\text{H}_2\text{O})]$ was demonstrated in Fig. 5. In the cyclic voltammogram the i_{pa} increased linearly on raising the sweep rate ($v^{1/2}$) indicating that, the electrochemical oxidation process is diffusion controlled electrochemical process [24].

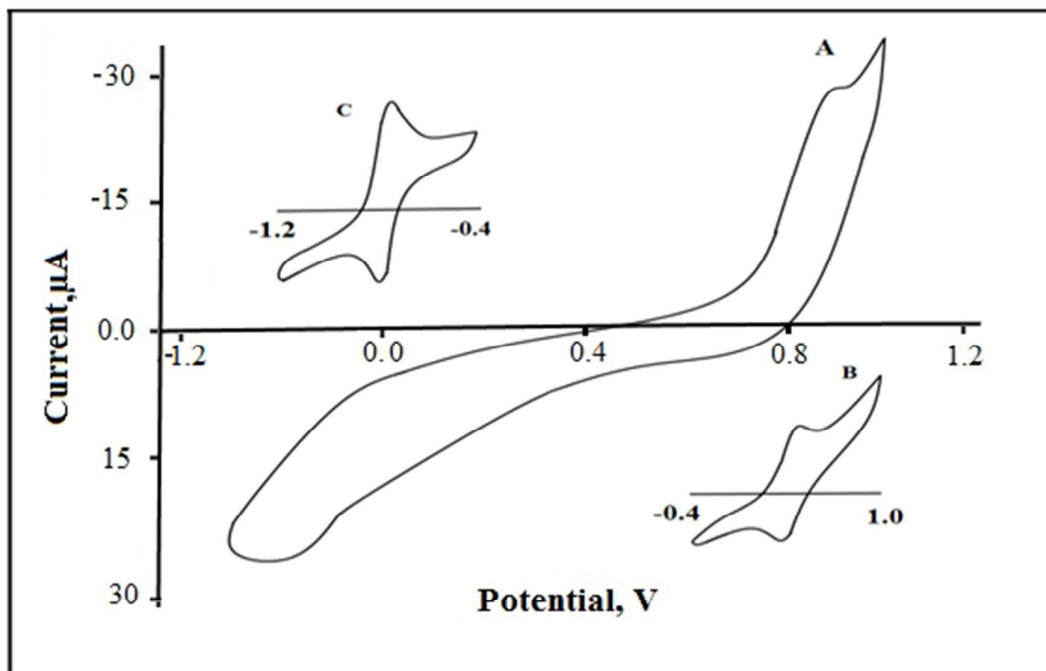


Fig. 5 Cyclic voltammograms of the complex $[\text{Ni}(\text{HHyMBPT})(\text{OH})(\text{H}_2\text{O})]$ in $\text{TBA}^+\text{BF}_4^-$ -DMF at 100 mVs^{-1} scan rate in the potential range $-1.2 - +1.2$ (A); $0.4 - 1.0$ (B) and $-1.4 - -0.4$ V (C) vs. Ag/AgCl reference electrode at 298 K.

The one electron nature of $\text{Ni}^{2+}/\text{Ni}^+$ couple was also confirmed from the CPC data. The couple with E_{pa} ($0.80 - 1.14$ V) and E_{pc} ($0.51 - 0.83$ V) with $\Delta E_{\text{p}} = 0.12 - 0.39$ V vs. Ag/AgCl was safely assigned to the irreversible $\text{Ni}^{2+}/\text{Ni}^{3+}$ (with $E_{1/2}$ values from -0.48 to -1.25 V) couple by comparison with similar nickel(II) analogous [34, 35]. The observed trend of $\text{Ni}^{2+}/\text{Ni}^+$ in nickel(II) complexes can be explained by adding (or withdrawing) one electron as shown for $[\text{Ni}(\text{HHyMBPT})(\text{OH})(\text{H}_2\text{O})]$ in Fig. 6. The plot of E_{pc} vs. $\log v$ was linear supporting the irreversible nature of the couples. CPC measurement at fixed potential

corresponding to the second oxidation peak (Couple II) showed one electron transfer/one nickel center corresponding to $\text{Ni}^{2+}/\text{Ni}^{3+}$ [34, 35].

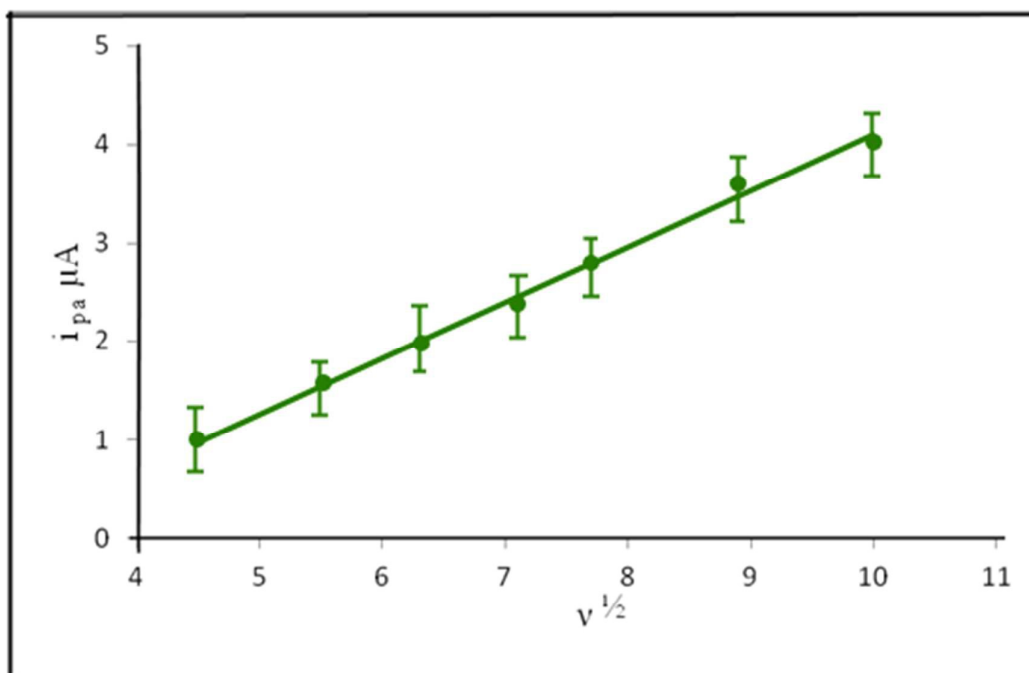


Fig.6. The plot of $i_{p,a}$ vs. square root of the sweep rate (v) of the couple $\text{Ni}^{2+}/\text{Ni}^{3+}$ of the complex $[\text{Ni}(\text{HHyMBPT})(\text{OH})(\text{H}_2\text{O})]$.

The irreversible nature of the observed electrode couples was further confirmed from the dependency of the linear plot of the E_{pc1} and E_{pc2} potentials vs. $\log v$. The charge transfer coefficient (α) and the product of the number (n) of electrons i.e. αn_a of the redox species involved in the reduction step can be computed from the slope of the linear plot of $E_{p,c}$ vs. $\log v$ (Fig. 3) employing the following equation:

$$\Delta E_{pc} / \Delta \log v = - 29.58 / \alpha n \quad (3)$$

For the couple $\text{Co}^{2+}/\text{Co}^+$ and assuming $n=1$, the computed value of α from the slope of the linear plot of E_{pc} vs. $\log v$ (Fig. 3) was found equal 0.59 confirming the irreversible nature of the couple [42, 43]. On the other hand, the ΔE_p of the $\text{Ni}^{2+}/\text{Ni}^{3+}$ couple also shifted towards

more negative and also on raising the sweep rate (v). This added further support to the irreversible nature and slow chemical reaction [41]. Thus, it can be concluded that, the species that initially formed may react further to give other Ni^{2+} complex products that are not re-oxidized at the same potential as in the first formed species of $\text{Ni}^{2+}/\text{Ni}^{3+}$ couple [24, 39,41].

The substituents on the thiosemicarbazone moiety (Table 3) have significant effect on the values of E_{pa} and E_{pc} of the couples $\text{Ni}^+/\text{Ni}^{2+}$ and $\text{Ni}^{2+}/\text{Ni}^{3+}$. The methoxy group on the complex $[\text{Ni}(\text{HHyMBPT})(\text{OH})(\text{H}_2\text{O})]$ decreases the ability of $\text{Ni}^{2+}/\text{Ni}^+$ couple to be oxidized whereas the $p\text{-ClC}_6\text{H}_4$ group in the $[\text{Ni}(\text{H}_2\text{SpClIPT})(\text{OAc})_2(\text{H}_2\text{O})]$ (Table 3) increases the ability of $\text{Ni}^{3+}/\text{Ni}^{2+}$ couple to be reduced. Similar behavior was also noticed on comparing $[\text{Ni}(\text{HHyMBPT})(\text{OH})(\text{H}_2\text{O})]$ with $[\text{Ni}_2(\text{H}_2\text{HyMBpClIPT})(\text{OAc})_4(\text{H}_2\text{O})_3]$ and $[\text{Ni}(\text{H}_2\text{SpClIPT})(\text{OAc})_2(\text{H}_2\text{O})]$ with $[\text{Ni}(\text{SET})(\text{H}_2\text{O})]1.5\text{H}_2\text{O}\cdot\text{C}_2\text{H}_5\text{OH}$. The group $p\text{-ClC}_6\text{H}_4$ stabilized nickel(I) species, while the NH_2 or $\text{C}_2\text{H}_5\text{NH}$ group favor oxidation to Ni^{3+} species. The complex species containing the electron attracting group $p\text{-ClC}_6\text{H}_4$ decreases the electron density at the reduction center. Thus, it become more positively charged and more easily to be reduced to nickel(I) species [37, 41]. On contrary, group e.g. NH_2 or $\text{C}_2\text{H}_5\text{NH}$ makes the complexes less positively charged and more easily to be oxidized to Ni^{3+} species.

The E_{pa} and E_{pc} values of the couple $\text{Ni}^{2+}/\text{Ni}^+$ of the complexes were slightly sensitive to substituent on N^4H and ligand pK_a . The fact that, the change of the coordination number of the metal ions upon the redox potentials may account for the observed trend [39]. The E_{pc} and E_{pa} peaks are from different chemical species i.e. are not to the complexes of interest and are undefined chemically as reported [39] and the chemical kinetics involved in the electron transfer process may account for the trend observed. Electron withdrawing group ($p\text{-ClC}_6\text{H}_4$)

stabilizes Ni⁺ complexes, while electron-donating group (NH₂ or C₂H₅NH) favors oxidation to Ni³⁺ species.

Table. 3 Electrochemical data of nickel (II) complexes in TBA⁺BF₄⁻-DMF at 100 mVs⁻¹*

Complex	Electrode couple, I			Electrode couple, II		
	E _{pa}	E _{pc}	ΔE _p	E _{pa}	E _{pc}	ΔE _p
[Ni(AT) ₂] ₂ H ₂ O	-1.12	-1.39	0.27	1.28	0.94	0.34
[Ni(AET) ₂]	-0.80	-1.20	0.40	1.19	1.14	0.05
[Ni ₂ (APT) ₃ (OH)(H ₂ O)]H ₂ O	-0.20	-0.78	0.58	0.86	0.78	0.08
[Ni(ApCIPT) ₂]	-0.72	-1.08	0.36	1.20	0.98	0.22
[Ni(HST)(OAc)]	-0.67	-1.08	0.41	0.87	0.75	0.12
[Ni(SET)(H ₂ O)]1.5H ₂ O.C ₂ H ₅ OH	-0.65	-1.07	0.42	0.80	0.51	0.29
[Ni(HSPT)(OAc)(H ₂ O) ₂]	-0.60	-1.08	0.48	1.12	0.83	0.29
[Ni(H ₂ SpCIPT)(OAc) ₂ (H ₂ O)]	-0.62	-1.09	0.47	0.96	0.73	0.23
[Ni(HHyMBPT)(OH)(H ₂ O)]	-0.51	-0.82	0.31	1.14	0.83	0.31
[Ni ₂ (H ₂ HyMBpCIPT)(OAc) ₄ (H ₂ O) ₃]	-0.04	-0.83	0.79	0.95	0.56	0.39
[Ni(BT)(OAc)(H ₂ O) ₂]H ₂ O	-0.12	-0.78	0.66	0.74	0.62	0.12

*ΔE_p = E_{pc} - E_{pa}

The E_{pa} and E_{pc} of the couple Ni²⁺/Ni⁺ of the complex [Ni(AT)₂]₂H₂O and [Ni(ApCIPT)₂] are more sensitive to the changes in the nucleophilic properties of the N¹H moiety; where ΔpK_a = 2.57 is associated with an increase of E_{pa} and E_{pc} of Ni⁺/Ni²⁺ couple. For Ni²⁺/Ni³⁺ couple of [Ni(ApCIPT)₂] and [Ni(H₂SpCIPT)(OAc)₂(H₂O)] , the same trend was also noticed where, when ΔpK_a was 2.57, an increase in the E_{pc} and E_{pa} was achieved (Table 3) in agreement with the results reported for Ru³⁺/Ru²⁺ couple [43, 44]. The spherical potential generated by the electron density of the donor atoms and the anti-bonding d-orbital's may account for the observed trend [33]. Thus, complexes of ligands having high electron density on their donor atoms (high pK_a) showed lower the E_{pc} and E_{pa} values than those of weaker bases. The plot of the Hammett constants (σ) of the substituents in N¹H or N⁴H moiety vs. E_{pc} and E_{pa} of the

couple $\text{Ni}^{2+}/\text{Ni}^+$ or $\text{Ni}^{2+}/\text{Ni}^{3+}$ revealed evidence of the substituents in N^1H or N^4H moiety on the values of E_{pa} and E_{pc} where the slope of the linear plot in most cases was > 0.1 [43].

3.3. Influence of ligand pK_a and d^n electron on the E_{pc}

The variations of the E_{pc} values of the couples M^{2+}/M^+ ; $\text{M}^{2+}/\text{M}^{3+}$ (where $\text{M} = \text{Co}, \text{Ni}$ or Cu) [23] may also be correlated with the nature of orbital's involved in the redox processes [27]. HOMO orbital is consisting predominately of dx^2-y^2 orbital while LUMO consisting of the anti-bonding π - orbital of the thiosemicarbazone moiety. Thus, the low values of E_{pc} for $\text{Ni}^{2+}/\text{Ni}^+$ couple and the high values for $\text{Ni}^{2+}/\text{Ni}^{3+}$ (Table 3) couple compared to $\text{Co}^{2+}/\text{Co}^+$ and $\text{Co}^{2+}/\text{Co}^{3+}$ couples (Table 2) and $\text{Cu}^{2+}/\text{Cu}^+$ and $\text{Cu}^{2+}/\text{Cu}^{3+}$ [27] of the same ligand can be explained in terms of the higher energy of $d x^2 - y^2$ orbital in nickel (II) compared to cobalt (II) and copper(II), respectively. These data are in good agreement with the data reported for Pd^{2+} and Pt^{2+} complexes [45,46]. The different extent of the back bonding from $d \pi$ - orbital of the metal to the anti bonding π - orbital of the corresponding ligand may also account for the observed behavior [46, 47].

The influence of pK_a of the ligands (Table 1) and d^n electron of metal ions of t_{2g} configuration was also studied. The plots of d^n electrons for Co^{2+} , Ni^{2+} and Cu^{2+} complexes of the same ligand and geometry *versus* E_{pa} and E_{pc} for the couple M^+/M^{2+} are shown in Figs. 7 and 8. Good correlation between E_{pa} and E_{pc} values of the complexes and d^n electrons in metal ions was noticed. The energy difference arising from the interaction between the non-bonding d^n electrons of the metal ion and the lone pair electrons of the coordinating sites of the Schiff base may account for the observed trend [38, 47]. This interaction raises the energy of t_{2g} metal HOMO electrons [48]. Based on the results given in Tables 2 and 3 and the data reported for other copper (II) complexes of the same ligands [28, 29], it can be concluded that, ligand of $pK_a = 12.39$ enforced metal ions to be oxidized in the following order:



Probably, the steric of electron-donating group at the reduction center hindered the approach of reduced centre to the electroactive surface [46, 47]. Thus, metal ions of high d^n electrons have E_{pc} lower than metal ions of low d^n electrons in the complexes i.e. the more the number of d electrons the less reduction on the electrode surface. Ligand of $pK_a = 10.8$ also enforced metal ions to be reduced in the order: $\text{Co}^{2+} > \text{Ni}^{2+} > \text{Cu}^{2+}$. Thus, high value of E_{pc} and E_{pa} for $\text{Co}^{2+}/\text{Co}^{3+}$ couple compared to $\text{Ni}^{2+}/\text{Ni}^{3+}$ or $\text{Cu}^{2+}/\text{Cu}^{3+}$ couples of the same ligand was explained in terms of higher energy of $d\ x^2-y^2$ orbital in Ni^{2+} or Cu^{2+} than in Co^{2+} [45, 47]. Thus, Co^{2+} ions became more positively charged and more difficult to be oxidized.

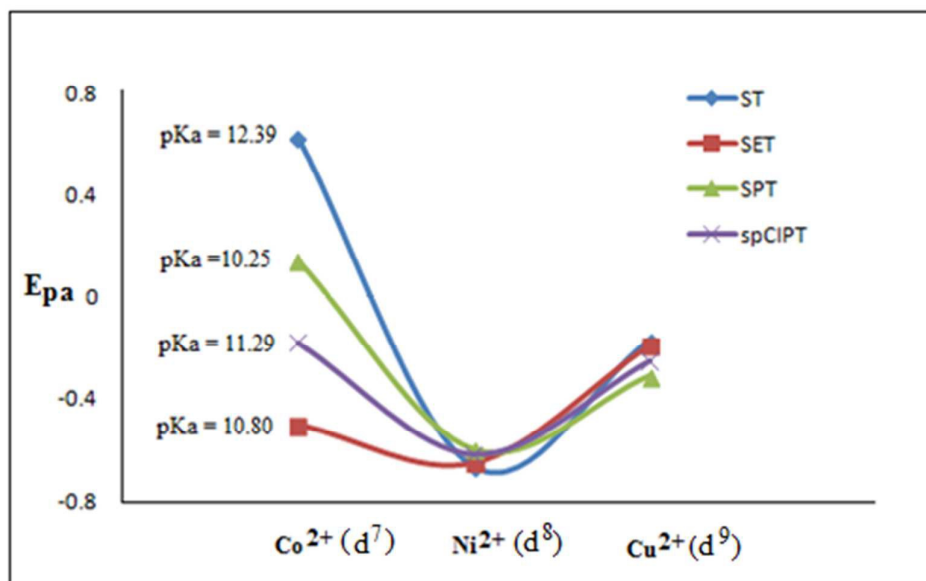


Fig. 7 Plots of E_{pa} of the electrode couple M^+/M^{2+} ($M = \text{Co}, \text{Ni}$ or Cu) vs. d^n -electrons of selected complexes.

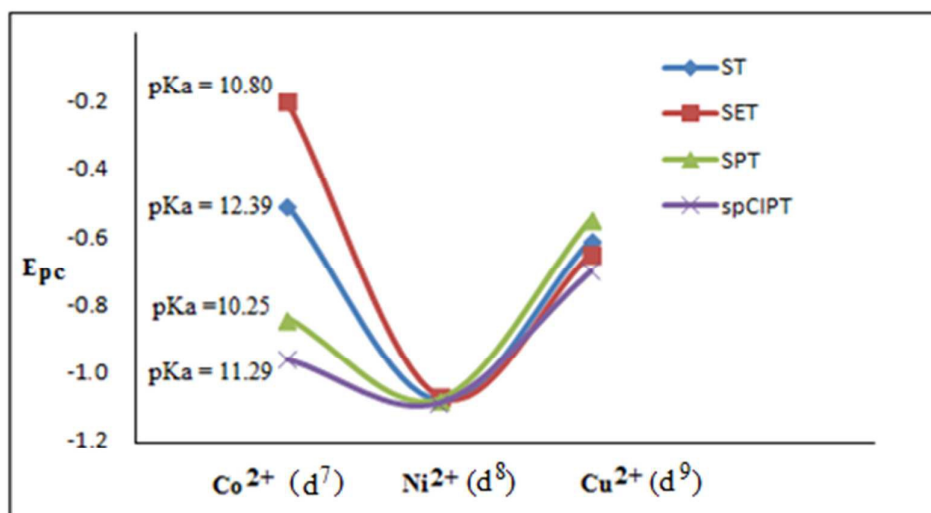


Fig. 8 Plots of $E_{p,c}$ of the electrode couple M^+/M^{2+} ($M = \text{Co}, \text{Ni}$ or Cu) vs. d^n -electrons of selected complexes

3.4. Energy levels approximation by cyclic voltammetry

Energy level characterization i.e HOMO/LUMO approximations were successfully computed for some of the Co^{2+} , Ni^{2+} and Cu^{2+} complexes. The optical band gap energy was calculated from the electronic spectra of each complex. The cross point of absorption onset line and corrected base line was used to calculate energy band gap [49]. The HOMO and LUMO processes are calculated from the cyclic voltammogram from their respective oxidation onset and reduction onset potentials. The equations including the value of ferrocene -4.4 were used as following [50]:

$$E(\text{HOMO}) = -e [E_{\text{ox}}^{\text{onset}} + 4.4] \quad (4)$$

The optical energy band gap was calculated using the following equation from the longest absorption wavelength λ_{onset} :

$$E_g = 1242/\lambda_{\text{onset}} \quad (5)$$

The combination of these two methods would deduce the feasibility of donor-acceptor system. The HOMO/LUMO energy levels and optical band gap energy are deduced using the

equations 3-5 as summarized in Table 4. As shown in Table 4 the transition of an electron from HOMO to LUMO upon photo-excitation at LUMO of the acceptor would eventually be collected at the respective electrode. This phenomenon is attributed to the fact that the excitation binding energy is lower than the electron affinity of the acceptor and potential difference between ionization potential of the donor. These characterizations would estimate whether the materials are suitable for use in photovoltaic devices and solar cells.

Table. 4 Calculation of optical band gap energies and excitation binding energies from electronic spectra and cyclic voltammetry

Complex	E_{ox}^0 (V) Ag/AgCl (V)	E_{ox}^0 onset vs. Ag/AgCl (V)	HOMO level (eV)	E_{red}^0 (V) Ag/AgCl (V)	LUMO level (eV)	Optical Energies (Eg)
[Co(APT) ₂ (H ₂ O) ₂]	-0.22	-0.03	4.37	-0.67	2.54	1.83
[Co ₂ (SET) ₂] ₂ C ₂ H ₅ OH	-0.20	-0.05	4.35	-0.26	2.75	1.6
[Co(HyMBPT)(H ₂ O) ₃] ₂ H ₂ O	-0.30	-0.20	4.2	-0.36	2.55	1.65
[Ni(HSPT)(OAc)(H ₂ O) ₂]	-0.60	-0.52	3.88	-1.08	1.33	2.55
[Ni(H ₂ SpCIPT)(OAc) ₂ (H ₂ O)]	-0.62	-0.55	3.85	-1.09	1.72	2.13
[Cu(AT)(OH)(H ₂ O) ₃]	-0.25	-0.43	3.97	-0.6	2.3	1.67

4. Conclusion

Substituents on the thiosemicarbazone moiety (N¹H and/or N⁴H) have significant effect on the redox properties of the redox couples (M²⁺/M⁺ and M²⁺/M³⁺). Co²⁺ or Ni²⁺ chelates undergo single one electron reduction and oxidation to the corresponding M⁺ and M³⁺

species, respectively. No significant variations in the D values on raising the concentrations of the complex species in solution. The changes in $E_{1/2}$ for the copper (II) complexes are strongly related to changes in the nucleophilic properties of substituents on C=N1 and N⁴H (Table 2, 3). Furthermore, the values of $E_{1/2}$ for the couples CuI/CuII and CuII/CuIII suggest that these couples are more sensitive to changes in the nucleophilic parameters of the N₄H substituents than the changes in C=N1 derivatives. The correlation between $E_{1/2}$ of the complexes and the pK_a of the ligands involved has been attributed to the spherical potential generated by the electron density of the donor atoms in the anti bonding d orbital's as reported by Lintvedt and Fenton [33]. Most of published Schiff base metal complexes of Co, Ni and Cu suffer from many drawbacks e.g. no correlation on the influence of metal ion dⁿ electrons and pK_a of the Schiff base on the E_{pc} of the redox couples, while in the present manuscript a correlation between the redox characteristics of the complexes with differently substituted of the thiosemicarbazone moiety N¹H and/ or N⁴H was noticed. The redox potentials are also not simply related to the pK_a values of the ligands (pK_a). Excitation energies i.e HOMO/LUMO and optical band gap energies were successfully computed for some of the Co²⁺, Ni²⁺ and Cu²⁺ complexes. The difference between the potentials of the redox couples and the absorption band energy for irreversible electron transfer processes is most likely assigned to the thermodynamic and kinetics parameters. The work is continuing for studying the spectroelectrochemical behavior of the various redox couples at optically transparent thin layer electrochemical cell.

5. References

- [1] A.A. Nejo, G.A. Kolawole and A.O. Nejo, *J. Coord. Chem.* 2010, **63**, 4398-4410.
- [2] W. Jiangtao and W. Hedong, *Inter.J. Biol. Macromolec.* 2011, **48**, 523-529.
- [3] A. S. El-Tabl, M. M. Abd-El Wahed, M. A. Wahba, Mohamad, M. E. Shakdofa and M. H. H. Abu-Setta, *J. Chem. Biol. Phys. Sci.*, 2015, **5**, 3697-3720.
- [4] S. Sathiyaraj, G. Ayyannan and C. Jayabalakrishnan, *J. Serb. Chem. Soc.* 2014, **79**, 151-165.
- [5] A.N. Kursunlu, E. Guler, F. Sevgi and B. Ozkalp, *J. Mol. Struct.* 2013, **1048**, 476-481.
- [6] J. Gao, Y. Guo, J. wang, Z. wang, X. Jin, C. Cheng, Y. Li and K. Li, , *Spectrochim. Acta A* 2011, **78**, 1278-1286.
- [7] M.A. Neelakantan, F. Rusalraj, J. Dharmaraja, S. Johnsonraja, T. Jeyakumar and M. Sankaranarayana Pillai, *Spectrochim. Acta A* 2008, **71**,1599-1609.
- [8] C. Anitha , C.D. Sheela, P. Tharmaraj and S. Johnson Raja, *Spectrochim. Acta A* 2012, **98**, 35-42.
- [9] S. Oz , J. Titiš, H. Nazır, O. Atakol, R. Boc̣a, I. Svoboda and H. Fuess, *Polyhedron* 2013, **59**, 1-7.
- [10] M. Kalita, T. Bhattacharjee, P. Gogoi, P. Barman, R. D. Kalita, B. Sarma and S. Karmakar, *Polyhedron* **60**, 2013, 47-53.
- [11] D. Kara, A. Fisher and S. J. Hill, *J. Hazard. Mater.* 2009, **165**, 1165-1169.
- [12] C. Praveen, K. Hemanth Kumar, D. Muralidharan and P.T. Perumal, *Tetrahedron* 2008, **64**, 2369-2374.
- [13] S.M. Abdallah, G.G. Mohamed, M.A. Zayed and M.S. Abou El-Ela, *Spectrochim. Acta A* 2009, **73**, 833-840.

- [14] K. Brodowska, I. Correia, E. Garribba, F. Marques, E. Klewicka, E. Łodyga-Chruscińska, J.C. Pessoa, A. Dzeikala and L. Chrusciński, *J. Inorg. Biochem.* 2016, **165**, 36-48.
- [15] J. Madhavan, E. Kavitha, S. Selvakumar and A. Chitra, *IOSRD Int. J. Phys.* 2016, **2**, 1.
- [16] L. Feng, W. Shi, J. Ma, Y. Chen, F. Kui, Y. Hui and Z. Xie, *Sens. Actuator B* 2016, **237**, 563-569.
- [17] M. Maddireddy, A.D. Kulkarni, G.B. Bagihalli and S. Malladi, *Helv. Chim. Acta* 2016, **99**, 562-572.
- [18] M. Cañadas, E. López-Torres, A. Martínez-Arias, M. A. Mendiola and M. T. Sevilla, *Polyhedron* 2000, **19**, 2059-2065.
- [19] R. M. El-Shazly, G. A. A. Al-Hazmi, S. E. Ghazy, M. S. El-Shahawi and A. A. El-Asmy, *Spectrochim. Acta A* 2005, **61**, 243-251.
- [20] G. A. A. Al-Hazmi, M. S. El-Shahawi, I. M. Gabr and A. A. El-Asmy, *J. Coord. Chem.* 2005, **58**, 713-733.
- [21] N.M. El-Metwally and A. A. El-Asmy, *J. Coord. Chem.* 2006, **59**, 1591-1601.
- [22] S. I. Mostafa, A. A. El-Asmy and M. S. El-Shahawi, *Transition Met. Chem.* 2000, **25**, 470-476.
- [23] A. A. El-Asmy, E. M. Saad and M. S. El-Shahawi, *Transition Met. Chem.* 1994, **19**, 406-408.
- [24] M. S. El-Shahawi, G. A. A. Al-Hazmi and A. A. El-Asmy, *Transition Met. Chem.* 2005, **30**, 464-470.
- [25] A. A. El-Asmy, I. M. Gabr, M.H. Abdelrahman and M.M. Hassenin, *J. Sulfur Chem. I* 2010, 141-151.
- [26] S. Durmus, A. Atahana and Mustafa Zengin, *Spectrochim. Acta A* 84, 2011, **84**, 1-5.
- [27] M.S. El-Shahawi and W.E. Smith, *Analyst* 1994, **119**, 327-331.

- [28] A.J. Bard and L.R. Faulkner, *Electrochemical Methods: Fundamentals and Applications*, John Wiley & Sons, Inc., 2000, Chapter 12.
- [29] R.S. Nicholson and I. Shain, *Anal. Chem.* 1964, **36**, 709-723.
- [30] D.T. Sawyer, W.R. Heinemann and J.M. Beebe, John Wiley & Sons, 1984.
- [31] C. A. Bowmaker, P. D. W. Boyd, G. K. Campbell, J. M. Hope, R. L. Martin, *Inorg. Chem.* 1982, **21**, 1152-1159.
- [32] S.M. Cohen, B.O'Sullivan and K.N. Raymond, *Inorg. Chem.* 2000, **39**, 4339-4346.
- [33] R. L. Lintvedt and D.E.Fenton, *Inorg. Chem.* 1980, **19**, 569-571.
- [34] N.C. Paramanik and S. Bhattacharya, *Polyhedron* 1997, **16**, 1755-1761.
- [35] M.C. Huges and D.J. Macero, *Inorg. Chem.* 1974, **13**, 2739-2744.
- [36] A.S.N. Murthy and K.S. Reedy, *Faraday Trans. 1* 1984, **80**, 2745-2750.
- [37] H. Lund, *Acta Chem. Scand.* 1959, **13**, 249-267.
- [38] M. Armando, R. Lena, M. Rafall and D. Federico, *J. Coord. Chem.* 1993, **29**, 359-370.
- [39] B.R. James and R.J.P. Williams, *J. Chem. Soc.* 1961, 2007-2019.
- [40] G.M. Abou-Elenien, N.A. Ismail, M.M. Hassanin and A.A. Fahmy, *Can.J. Chem.* 70 (1992) 2704-2708.
- [41] G. M. Abdou-Elenien, N. A. Ismail, M. M. Hassanin and A. A. Fahmy, *Can. J. Chem.* 1992, **70**, 2704-2708.
- [42] B.S. Parajoin-Costa, A.C. Gonzalez-Baro and E.J. Baran, *Anorg. Allg. Chem.* 2002, **628**, 1419-1424.
- [43] L. M. Araya, J. A. Vargas and J. A. Costamagna, *Transition Met. Chem.* 1986, **11**, 312-316.
- [44] P. Zuman, *Substituent Effects in Organic Polarography*, Plenum Press, New York, 384 (1967).
- [45] W. A. Leung and C. M. Che, *Inorg. Chem.* 1989, **28**, 4619-4622.

- [46] R. H. Morris, *Inorg. Chem.* 1992, **31**,1471-1478.
- [47] W. L. Jolly, *Modern Inorganic Chemistry*, McGraw-Hill, New York, (1984) 409.
- [48] S. K. Kamath, V. Uma and T. S. Srivastava, *Inorg. Chim. Acta*, 1989, **161**, 49-56.
- [49] A. Shafiee, M.M. Salleh, M. Yahaya, *Sains Malaysiana* 2011, **40**, 173-176.
- [50] L. Leonat, G. Sbârcea, I.V. Branzoi, *UPB Sci Bull Ser B* 2013, **75**, 111-118.